Everest Advances in Science and Technology (EAST), Vol. 1, No. 1, 2025
ISSN: 3102-0410(print), 3102-0429(online)

Modeling and Simulation of Single-Mass PMSG for Embedded Control in Wind Energy Systems

ANIL THAPA[1*]

Abstract. Accurate yet computationally efficient modeling is essential for the real-time control of Permanent Magnet Synchronous Generator (PMSG)-based wind energy conversion systems (WECS), particularly when targeting low-cost embedded platforms. Complex multi-mass drive-train models, while capable of capturing torsional dynamics, introduce significant computational overhead that can limit their applicability in rapid control prototyping and embedded implementations. This paper presents a complete single-mass PMSG model derived from aerodynamic, mechanical, and electrical subsystems, expressed in the d-q reference frame for efficient control integration. The modeling approach consolidates the turbine and generator inertias into a single equivalent inertia, significantly reducing the system order while preserving the key dynamics necessary for steady-state and slow-transient analysis. The model is implemented in MATLAB/Simulink with fixed-step solver configurations to ensure compatibility with embedded hardware such as DSPs, FPGAs, and microcontrollers. Simulation results under variable wind speed conditions demonstrate the model's suitability for maximum power point tracking (MPPT) and DC-link voltage regulation. The proposed lightweight approach provides a balance between model fidelity and execution speed, making it ideal for cost-sensitive, real-time wind energy control applications.

Keywords: Wind energy, single mass, permanent magnet synchronous generator, MPPT.

[1]Department of Computer Engineering, Everest Engineering College, Sanepa, Lalitpur, Nepal
E-mail: bineilthapa@gmail.com
* Corresponding author
Manuscript received: 12 March, 2025; revised: 21 August 2025; accepted: 4 September, 2025.
Everest Advances in Science and Technology (EAST), Vol. 1, No. 1, 2025

1. Introduction

The global warming effect is becoming more conspicuous every day. The lack of snows in the mountains to the wildfire happening around the world clearly substantiate this. Despite the emphasis on renewable energy sources, whole world is still heavily reliant on fossils fuels. Of all the available renewable resources, the wind energy has drawn increased attention [1, 2, 3]. In 2023, a record high 117 GW of new wind power was installed worldwide representing a 50% hike from the previous year [1].

Permanent magnet synchronous generator (PMSG) has been an attractive choice for applications requiring variable speed drives [4]. PMSGs are used in wind turbines for their high frequency and removal of gear box for electricity generation. PMSG transfers the total power generated at the generator side resulting from turbine to grid side with the help Back-To-back (BTB) capacitor which consists of a Machine Side Converter (MSC), dc link capacitor and Grid Side Converter (GSC) [5].

The rapid growth of wind energy has driven the development of efficient and flexible control strategies for variable-speed generators. Among various generator technologies, the Permanent Magnet Synchronous Generator (PMSG) has gained significant attention due to its high efficiency, gearless operation, and direct-drive capability. Accurate modeling of PMSG-based wind energy conversion systems (WECS) is essential for designing, testing, and validating control algorithms prior to deployment in hardware.

Conventional modeling approaches often employ multi-mass drive-train representations to capture torsional oscillations and shaft flexibility. While effective for detailed mechanical stress analysis and transient studies, such models increase system complexity, require additional mechanical parameters, and demand higher computational resources. These characteristics make them less suited for applications where real-time performance and low-latency control execution are critical, such as in embedded controllers with limited processing capacity.

In many scenarios—particularly small to medium-scale wind turbines, educational test benches, and rapid control prototyping environments—a reduced-order mechanical model can provide adequate accuracy with a fraction of the computational burden. This paper develops a mathematically complete single-mass PMSG model that consolidates the turbine and generator inertias into a single equivalent inertia. The model is derived from first principles, combining aerodynamic torque generation, single-mass mechanical dynamics, and electrical equations in the dq reference frame. Implemented in MATLAB/Simulink with fixed-step solver settings, the model is tailored for deployment to digital signal processors (DSPs), microcontrollers, and FPGA platforms.

2. System Model

Figure 1 gives the schematic of a PMSG driven by a wind turbine connected to the single machine infinite bus system (SMIB). Both MSC and GSC emulate the PWM signal generation using tip speed ratio maximum power point algorithm (MPPT). The dc link capacitor in back-to-back converter is responsible for power transfer between generation and grid side. On the generator side, rectifier utilizes tip speed ratio (TSR) MPPT algorithm for the maximum power delivery.

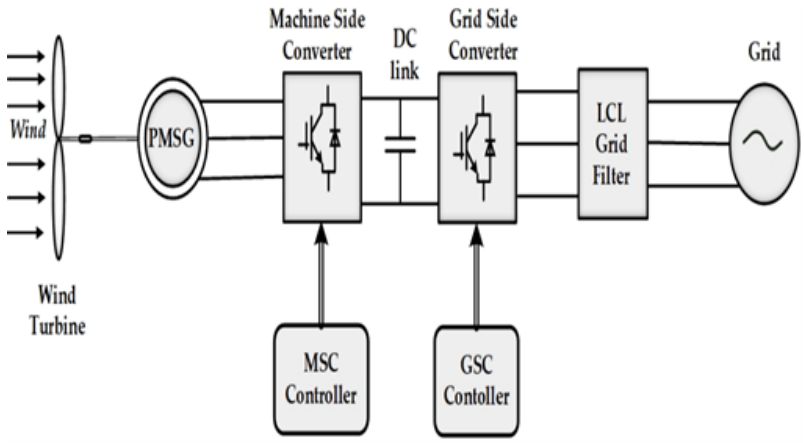

FIGURE 1. Schematic diagram of a. single machine infinite bus (SMIB) system using PMSG wind turbine system.

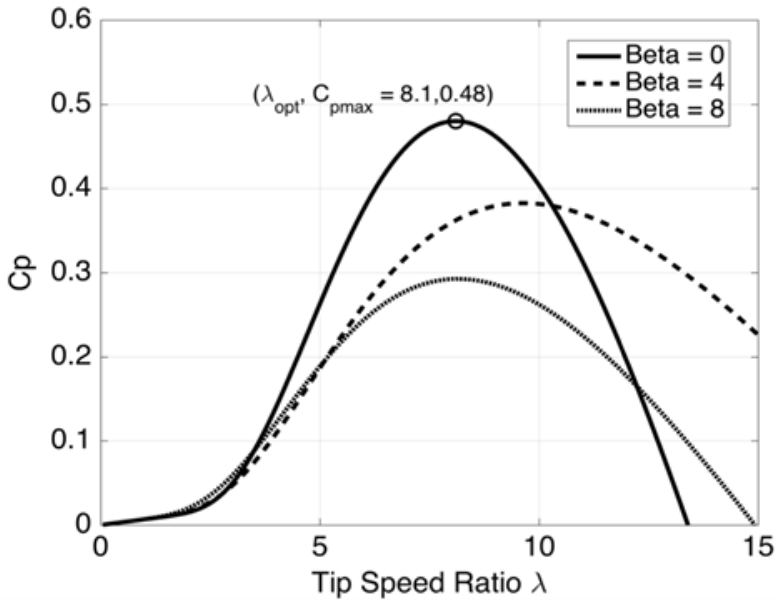

FIGURE 2. Tip speed ratio vs power coefficient curve for different pitch angles.

2.1. **Mechanical Drive Train.** The mechanical power output of a wind turbine is related to the wind speed V_ω by [6, 7, 8]:

$$P_t = 0.5\rho A C_p(\lambda, \beta) V_\omega^3 \tag{1}$$

where, ρ is air density, A is the area swept by the blades, and $C_p(\lambda, \beta)$ is the power coefficient of the blade which is given by

$$C_p(\lambda, \beta) = 0.5176 \left(\frac{116}{\lambda + 0.08\beta} - \frac{4.0}{1 + \beta^3} - 0.4\beta - 5 \right) e^{\left(\frac{-21}{\lambda + 0.08\beta} - \frac{0.735}{1+\beta^3} \right)} + 0.0068 \tag{2}$$

λ is the tip speed ratio and β is the pitch angle.

Figure 2 shows the variation of power coefficient with tip speed ratio for different values of pitch angle. C_p represents the fraction of wind power that can be extracted from the turbine. Pitch angle relates the orientation of the wind turbine blade with respect to its longitudinal axis. The extraction of wind energy is maximum when the blades are facing the wind. The pitch angle is zero degrees at this instance. The turbine power coefficient has a maximum value of 0.48 with the value of tip speed ratio around 8 as shown in Figure 2.
Because of the gearless configuration, the wind turbine system is connected to the generator with a single-mass model of the drive train. The dynamic equation representing the single-mass model of the drive train is expressed as:

$$p(\omega_t) = \frac{1}{2H}(T_m - T_e) \tag{3}$$

Here, ω_t, H, T_m, and T_e are the turbine speed, inertia constant, mechanical torque, and electrical torque, respectively.

2.2. **Permanent Magnet Synchronous Generator Model.** The electrical model of the PMSG in the synchronous reference frame can be expressed as [9]:

$$p(i_{sd}) = \frac{1}{L_d}\left[-R_a i_{sd} + \omega_g X_q i_{sq} - v_{sd}\right] \tag{4}$$

$$p(i_{sq}) = \frac{1}{L_q}\left[-\omega_g X_d i_{sd} - R_a i_{sq} + \omega_g \psi_{pm} - v_{sq}\right] \tag{5}$$

In the above, i_{sd}, i_{sq} and v_{sd}, v_{sq} are the d-q components of the stator current and terminal voltage respectively, and ψ_{pm} is the residual flux of the permanent magnet rotor.
The electrical torque generated is given by:

$$T_e = -L_d i_{sd} i_{sq} + \psi_{pm} i_{sq} + L_q i_{sd} i_{sq} \tag{6}$$

The active power at the PMSG terminal is given by:

$$P_{pmsg} = v_{sd} i_{sd} + v_{sq} i_{sq} \tag{7}$$

2.3. **Machine Side Converter Controller.** The decoupled control strategy is implemented in the MSC controller where the q-axis regulates torque and the d-axis regulates reactive power. The d-q axis is selected in such a way that $v_{sq} = |V|$ and $v_{sd} = 0$, so that the d-axis current reference becomes $i_{sd\_ref} = 0$.
The torque reference is obtained using MPPT and is given by:

$$T_e = k_{opt}\omega_t^2 = \psi_{pm} i_{sq} \tag{8}$$

Hence, the reference value of i_{sq} is:

$$i_{sq\_ref} = \frac{k_{opt}\omega_t^2}{\psi_{pm}} \tag{9}$$

The Simulink model representation of the MSC controller is shown in Figure 3. The blocks MSC_IL1 and MSC_IL2 each include two PI Controllers.

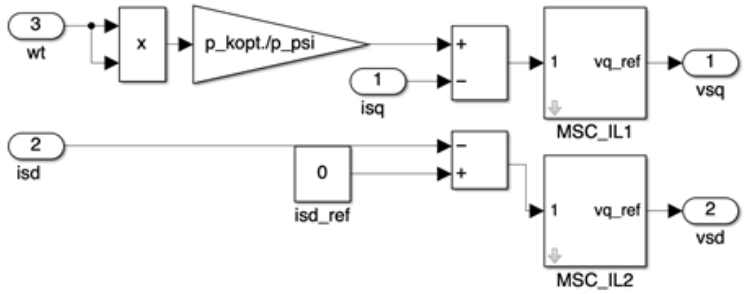

FIGURE 3. Simulink diagram of PMSG Machine Side Converter.

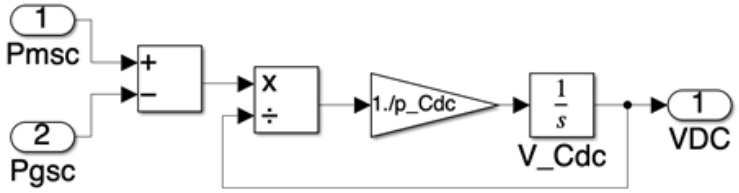

FIGURE 4. Simulink diagram of Back-to-back capacitor Converter.

2.4. **Back-To-Back Capacitor.** The Back-to-back converter consists of an MSC, a DC link capacitor, and a GSC. The losses due to switching of the converter are neglected. It is assumed that the converter dynamics are fast and the converter follows the reference generated by the MSC and GSC in real time.
The converter capacitor voltage is given by the power balance equation, excluding losses. The DC link capacitor voltage is:

$$V_c \left[C \frac{d}{dt}(V_c) \right] = P_{MSC} - P_{GSC} \tag{10}$$

Here, P_{MSC} and P_{GSC} are the power input and power output in the converter, given by:

$$P_{MSC} = V_{sd} i_{sd} + V_{sq} i_{sq} \tag{11}$$

$$P_{GSC} = V_{id} i_{id} + V_{iq} i_{iq} \tag{12}$$

2.5. **LCL Filter.** LCL filter consists of two inductors (L_i, L_g), a capacitor (C_f), and a damping resistor (R_C). The resistances (R_i, R_g) in series with the inductors represent the stray resistance of the inductors [10, 11]. Fig. 5 represents the structure of the LCL filter and Fig. 6 shows its Simulink representation.

The equations pertaining to the LCL filter are as follows:

$$p(i_{iq}) = \frac{w_b}{L_i} \left[v_{iq} - v_{cq} - (R_i + R_c) i_{id} + w L_i i_{id} + R_c i_{gq} \right] \tag{13}$$

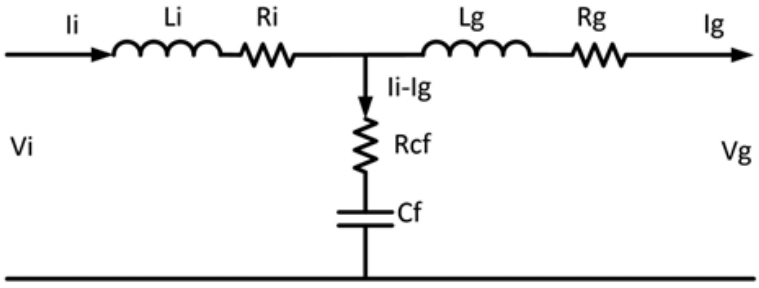

FIGURE 5. LCL filter.

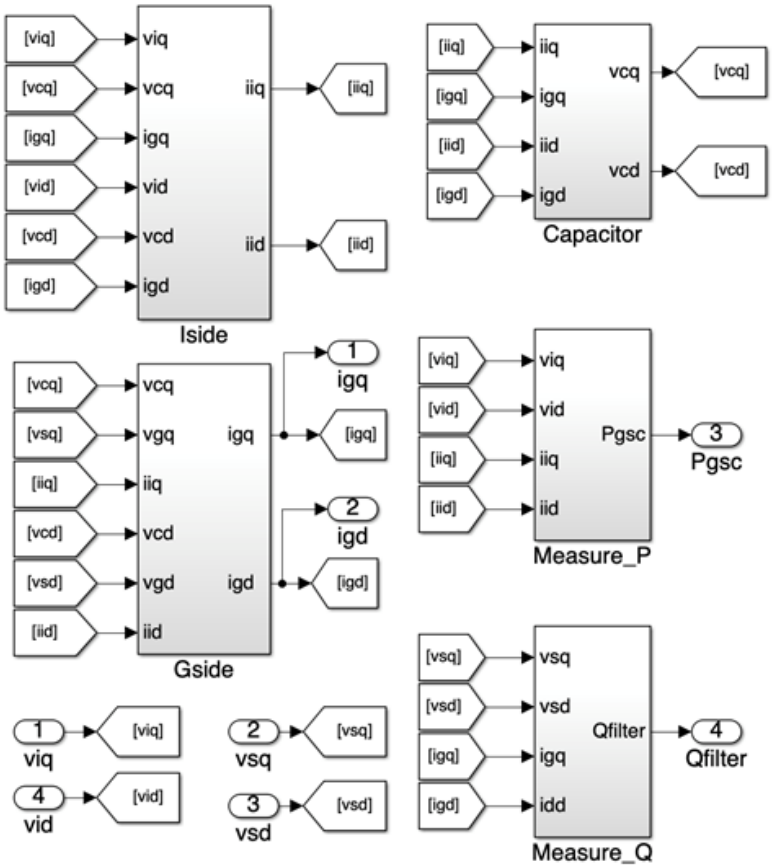

FIGURE 6. . Simulink representation of LCL filter.

$$p(i_{id}) = \frac{w_b}{L_i}\left[v_{id} - v_{cd} - (R_i + R_c)i_{id} - wL_i i_{iq} + R_c i_{gd}\right] \tag{14}$$

$$p(i_{gq}) = \frac{w_b}{L_g}\left[v_{cq} - v_{gq} - (R_g + R_c)i_{gq} + wL_g i_{gd} + R_c i_{iq}\right] \tag{15}$$

$$p(i_{gd}) = \frac{w_b}{L_g}\left[v_{cd} - v_{gd} - (R_g + R_c)i_{gd} + wL_g i_{gq} + R_c i_{id}\right] \tag{16}$$

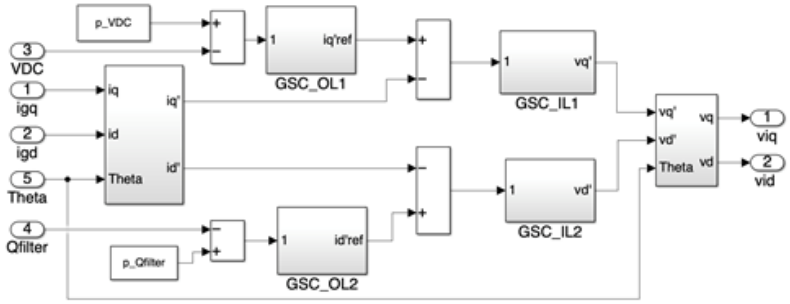

FIGURE 7. Simulink diagram of PMSG Gride Side Converter.

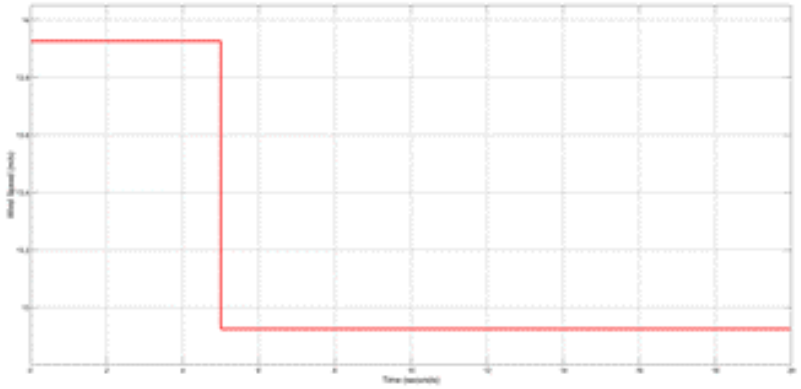

FIGURE 8. Variation in windspeed at time = 1s.

$$p(v_{cq}) = \frac{w_b}{C_f}\left[i_{iq} - i_{gq} - wC_f v_{cd}\right] \tag{17}$$

$$p(v_{cd}) = \frac{w_b}{C_f}\left[i_{id} - i_{gd} - wC_f v_{cq}\right] \tag{18}$$

2.6. **Grid Side Converter Controller.** Figure 7 shows the Simulink representation of the GSC controller, which consists of two inner PI controllers and two outer PI controllers. These controllers, along with the MSC controllers, are responsible for maintaining a constant DC voltage across the DC link capacitor, even when wind speed changes act as disturbances.

3. Simulation Results

The dynamic performance of the PMSG system is simulated using MATLAB SIMULINK. Figure 8 shows the dynamic simulations of the results by applying a step change in wind speed at time = 5s and infinite bus voltage change at time = 15s. It is clear from the figures that the controller performs satisfactorily with less overshoot and immediate stability for both the changes in wind velocity and infinite bus voltage. Moreover, the dc link voltage of the back-to-back capacitor is maintained constant with the overshoot value within the limit of 10% so that the peak overshoot won't damage the capacitor.

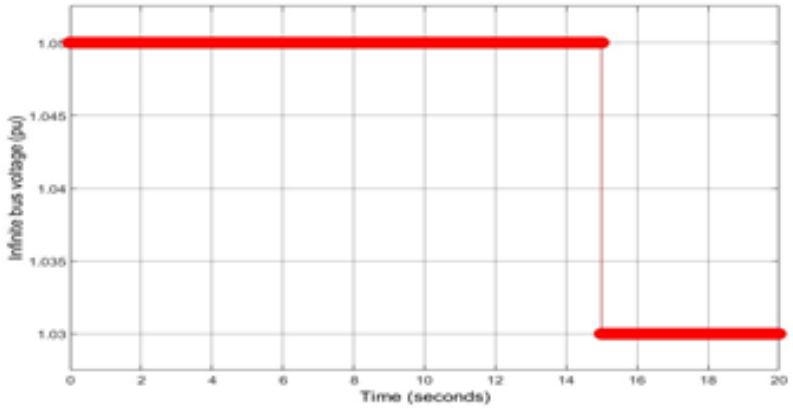

FIGURE 9. Variation in infinite bus voltage at time = 15s.

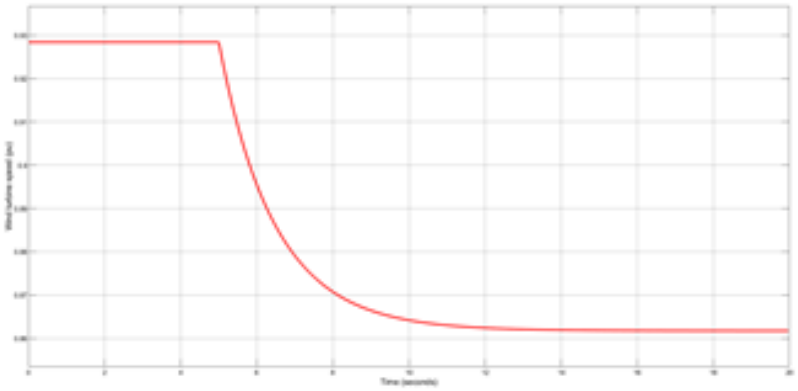

FIGURE 10. Variation in wind turbine speed following change in windspeed at time 5s and infinite bus voltage change at 15s.

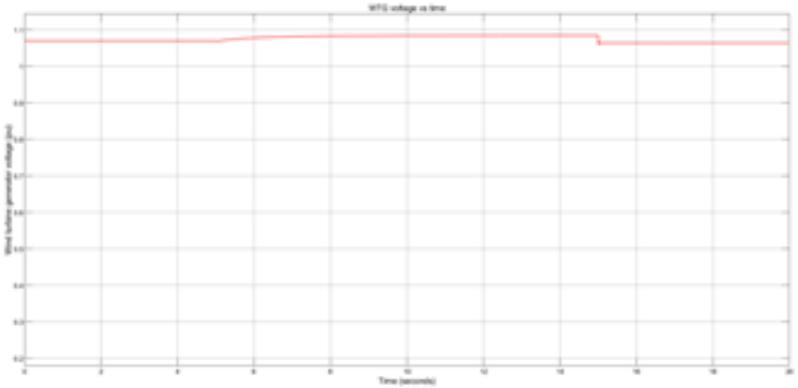

FIGURE 11. Variation in wind turbine generator voltage following change in windspeed at time 5s and infinite bus voltage change at 15s.

4. Conclusion

This paper presents a mathematically complete single-mass model of a Permanent Magnet Synchronous Generator (PMSG) wind energy system, integrating aerodynamic, mechanical, and electrical dynamics within a unified framework. The proposed model consolidates

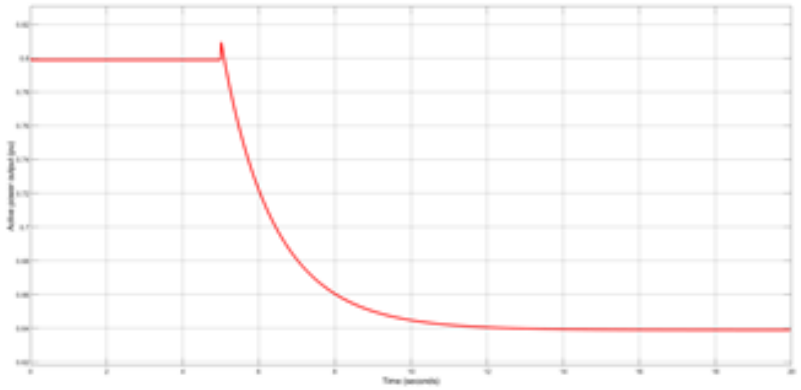

FIGURE 12. Variation in active power output following change in windspeed at time 5s and infinite bus voltage change at 15s.

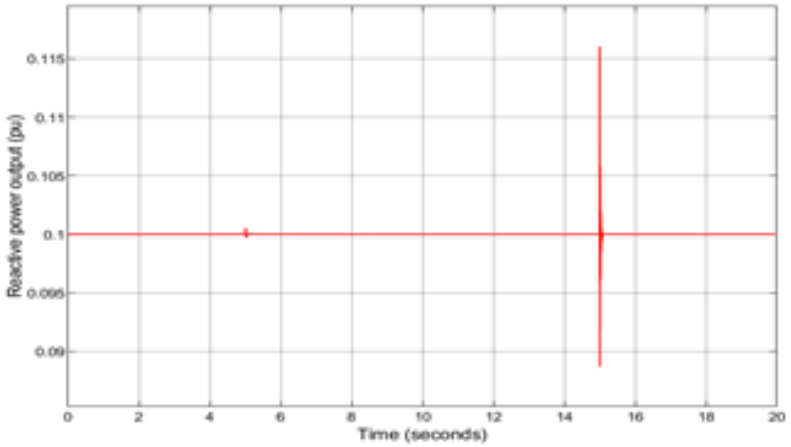

FIGURE 13. Variation in reactive power output following change in windspeed at time 5s and infinite bus voltage change at 15s.

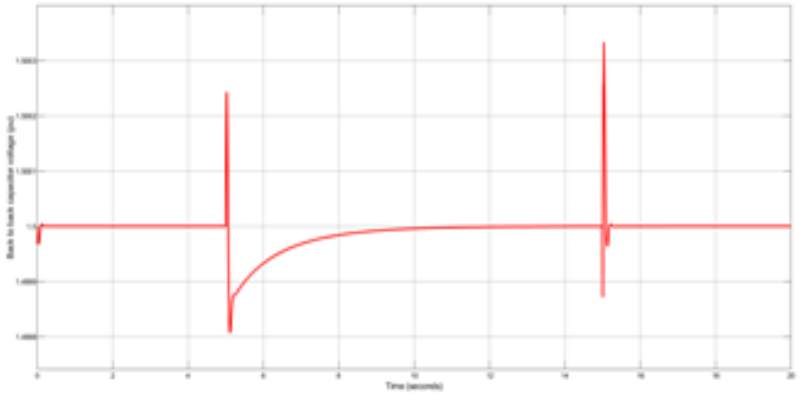

FIGURE 14. Variation in back-to-back capacitor voltage following change in windspeed at time 5s and infinite bus voltage change at 15s.

turbine and generator inertias into a single equivalent mass, significantly reducing computational complexity while preserving the essential dynamic behavior required for steady-state and slow-transient analysis. Implemented in MATLAB/Simulink with fixed-step solver configurations, the model is well-suited for embedded control applications, enabling real-time deployment on digital signal processors, microcontrollers, and FPGA-based platforms. Simulation results under varying wind conditions demonstrate that the single-mass model supports accurate maximum power point tracking (MPPT) and DC-link voltage regulation, while offering a lightweight alternative to more complex multi-mass representations. By balancing model fidelity and computational efficiency, this approach provides a practical framework for rapid prototyping, educational purposes, and cost-sensitive embedded wind energy systems. Future work may extend this model to include real-time hardware-in-the-loop (HIL) validation and integration with advanced control strategies such as fuzzy logic or reinforcement learning-based MPPT.

References

[1] R. Williams and F. Zhao, *Global Wind Report 2024*. Global Wind Energy Council (GWEC), 2024.

[2] E. Brunner and D. Schwegman, "Commercial wind energy installations and local economic development: Evidence from U.S. counties," *Energy Policy*, vol. 165, p. 112993, 2022.

[3] European Wind Energy Association, *Rewarding Ambition in Wind Energy: A Report*. Brussels, Belgium: EWEA, 2015.

[4] L. Barote and C. Marinescu, "PMSG wind turbine system for residential applications," in *Proc. Int. Symposium on Power Electronics, Electrical Drives, Automation and Motion (SPEEDAM)*, Pisa, Italy, Jun. 2010.

[5] B. Pal, S. Kuenzel, and L. Kunjumuhammed, *Simulation of Power System with Renewables*. Cambridge, MA, USA: Academic Press, 2020.

[6] W. Shepherd and L. Zhang, *Electricity Generation Using Wind Power*. Singapore: World Scientific, 2011.

[7] V. Akhmatov, *Analysis of Dynamic Behaviour of Electric Power Systems with Large Amount of Wind Power*. Ørsted-DTU, Technical Univ. of Denmark, 2003.

[8] H. Polinder, S. W. H. de Haan, M. R. Dubois, and J. G. Slootweg, "Basic operation principles and electrical conversion systems of wind turbines," *EPE J.*, vol. 15, pp. 43–50, 2005.

[9] S. Li, T. A. Haskew, and L. Xu, "Conventional and novel control designs for direct driven PMSG wind turbines," *Electr. Power Syst. Res.*, vol. 80, no. 3, pp. 328–338, Mar. 2010, doi: 10.1016/j.epsr.2009.09.016.

[10] M. Rosyadi, S. M. Muyeen, R. Takahashi, and J. Tamura, "New controller design for PMSG-based wind generator with LCL-filter considered," in *Proc. 20th Int. Conf. on Electrical Machines (ICEM)*, Marseille, France, Sep. 2012.

[11] R. L. A. Ribeiro, A. D. Araujo, A. C. Oliveira, and C. B. Jacobina, "A high-performance permanent magnet synchronous motor drive by using a robust adaptive control strategy," in *Proc. IEEE Power Electron. Specialists Conf. (PESC)*, Orlando, FL, USA, 2007.